Dip of the granular shear stress

Dmitry O. Krimer, Stefan Mahle, and Mario Liu
Theoretische Physik, Universität Tübingen, Auf der Morgenstelle 14, 72076 Tübingen, Germany
(Received 30 April 2012; published 17 December 2012)

Recent experiments reveal an unexpected dip of the shear stress as the shear rate increases, from the rate-independent regime to Bagnold flow. Employing granular solid hydrodynamics, it is shown that in uniform systems, such dips occur for given pressure or normal stress, but not for given density. If the shear rate is strongly nonuniform, enforcing a constant volume does not prevent the local density to vary, and a stress dip may still occur.

DOI: 10.1103/PhysRevE.86.061312 PACS number(s): 45.70.Vn, 45.70.Mg, 81.05.Rm, 81.40.Jj

I. INTRODUCTION

Granular materials are known to display a rich variety of interesting phenomena and to possess great significance for geophysics and industrial applications. Although these media (that we after all deal with in our daily life) appear simple and easily understandable, establishing a robust macroscopic understanding complete with a continuum mechanical theory has turned out to be a challenging task. For instance, only recently was it revealed, to the surprise of many in the field, that shear stresses display a nonmonotonic behavior as the shear rate increases. The first experiment is in a top-rotating torsional shear cell [1,2], the second in a split-bottom shear cell [3]. One difficulty in modeling a granular medium stems from its qualitatively different behavior in different rate regimes, depending on how strongly the grains are agitated. So less surprisingly, the stress dip occurs between two rate regimes, the rate-independent elasto-plastic one and that of rapid dense flow.

Elasto-plastic deformation has been under the focus of engineering research for many decades if not centuries [4–9]. The state of engineering theories, though typically confined to the rate-independent regime, remains highly confusing, at least for physicists: Innumerable continuum mechanical models compete, employing strikingly different expressions. Some are even proprietary, well hidden in codes. Nevertheless, all models yield a realistic account of the critical state and other uniform deformations, the better ones also of the shear band [10]. The second regime, rapid dense flow (such as heap flows, mud slides, or avalanches), is simply taken to obey different sets of equations [11–15].

A unified theory capable of accounting for granular phenomena of arbitrary shear rates, from static stress distribution at vanishing rates, over the rate-independent elasto-plastic motion at slow rates, to the rapid dense flow at high rates, would therefore seem a useful tool, both practically and to help build a sound, robust understanding of granular physics.

Granular solid hydrodynamics (GSH) is a continual mechanical theory derived from a few inputs that we hold to be the basic physics of granular media [16], and hence constructed to be broad ranged. Until now, GSH has shown itself capable of accounting for phenomena such as static stress distribution [17–19], incremental stress-strain relation [20], yield [21], propagation and damping of elastic waves [22], elasto-plastic motion [23], the critical state [24], and fast dense flow [25]. Clearly, whether the stress dip may be accounted for, at least qualitatively, is another useful test for GSH, especially because the effect was not anticipated.

An important ingredient of GSH is its set of state variables. In addition to the usual ones, density ρ, temperature T, and velocity v_i, GSH has two additional variables: the granular temperature T_g (or equivalently granular entropy s_g) and the elastic strain u_{ij}. The first is a measure for granular agitation and, similar to the true temperature T, a summary variable: T_g accounts for the energy w_T contained in the mesoscopic, intergranular degrees of freedom, the same as T accounting for the microscopic, inner granular ones. In other words, T_g accounts for the strongly fluctuating kinetic and elastic energy associated with granular jiggling. All this is typical of granular media, in which irreversibility and energy decay have two cascades: Energy always goes from the macroscopic to the mesoscopic, and on to the microscopic degrees of freedom, never backwards.

Accounting for high densities, when enduring contacts abound and granular jiggling is small, we expand w_T to obtain $w_T = s_g^2/(2\rho b)$, with $T_g \equiv \partial w_t/\partial s_g = s_g/\rho b$. The quadratic term is the lowest order one because $s_g, T_g = 0$ is an energy minimum, the same as in a Ginzburg-Landau expansion, just without the fourth order term or a phase transition. [The expansion coefficient b is defined in Eq (14d).] Note that the usual granular temperature T_G is defined as $2/3$ of a grain's average kinetic energy. This is useful in the dilute limit when there is little elastic energy in w_T. Then, and only then, does the relation (with m denoting the average mass of the grains) hold:

$$w_T = 3\rho T_G/2m = \rho b T_g^2/2. \tag{1}$$

Employing the strain rather than stress as a state variable yields a simpler description, because the former is in essence a geometric quantity, while the latter contains material parameters such as stiffness. Yet one cannot use the total strain field ε_{ij} of conventional elasticity, because its relation to the stress lacks uniqueness when the system is plastic. Engineering textbooks divide ε_{ij} into two symmetric fields, elastic u_{ij} and plastic $\varepsilon_{ij}^{(p)}$, with the first accounting for the reversible and second for the irreversible part. They then employ $\varepsilon_{ij}, \varepsilon_{ij}^{(p)}$ as two independent fields to account for granular elasto-plasticity. We believe one should, on the contrary, take the elastic strain u_{ij} as the sole variable. Interpreted as a coarse-grained measure of the grains' deformation, it relates uniquely to the elastic energy w_Δ and the elastic stress:

$$\pi_{ij} = -\partial w/\partial u_{ij};$$

see Ref. [16] for a rigorous derivation. More plausibly, this relation may be seen to hold because granular deformation results in a restoring force, the macroscopic expression of which is the elastic stress, and because u_{ij} is related to coordinates. (Deriving the energy with respect to the coordinate one obtains the force; one obtains the stress if the derivative is with respect to u_{ij}.) Note that the relation between the elastic and total strain is simple only at small increments, where $\delta u_{ij} = \delta\varepsilon_{ij}$ holds. More generally, it is given by the evolution equation of u_{ij}; see Sec II. Its basic structure is

$$\partial_t u_{ij} - v_{ij} = -u_{ij}/\tau,$$

where $v_{ij} \equiv \frac{1}{2}(\nabla_i v_j + \nabla_j v_i)$ is the strain rate. It accounts for the usual change of elastic deformation, while $-u_{ij}/\tau$ accounts for its relaxation. As this happens only when the grains jiggle and briefly lose contact with one another, we set $1/\tau \sim T_g$. [See Eq. (10) for the proper nonlinear convective derivative.]

Given the two additional variables, T_g and u_{ij}, the total stress σ_{ij} is fully determined by the necessity to comply with various general principles; see the discussion in Sec. II and Ref. [16]. It has three contributions: elastic π_{ij}, seismic $P_T\delta_{ij}$, and viscous $-\eta_g v^0_{ij}$ (with v^0_{ij} the traceless part of v_{ij}). The stress expression is given in Sec. II. For the discussion here, the following qualitative expression is sufficient:

$$\sigma_{ij} = \pi_{ij} + P_T\delta_{ij} - \eta_g v^0_{ij}. \tag{2}$$

At slow rates, in the rate-independent regime, only the elastic stress is important. Given an expression for the energy w (provided in Sec. II), π_{ij} is known, and we can use the force balance $\nabla_j\sigma_{ij} = \nabla_j\pi_{ij} = \rho g_i$ (with g_i the gravitational constant) to calculate static stress distributions [17–19]. We also can consider elasto-plastic motion [23] employing the evolution equation of u_{ij}, the stationary solution of which turns out [24] to be the critical state, $\sigma^{(c)}_{ij}(\rho)$, a rate-independent function of the density alone.

At higher rates, the seismic pressure P_T exerted by granular agitation and the viscous stress $-\eta_g v^0_{ij}$ also become important. They are

$$P_T = -\frac{\partial(w_T V)}{\partial V} = -\frac{\partial(w_T/\rho)}{\partial(1/\rho)} \sim T_g^2, \tag{3}$$

$$\eta_g = \eta_1 T_g, \quad T_g \sim v_s \equiv \sqrt{v^0_{ij}v^0_{ij}}. \tag{4}$$

$P_T \sim T_g^2$ is the usual fluid pressure exerted by grains jiggling and given by the energy $w_T \sim T_g^2$ derived with respect to the volume V. We therefore call it the *seismic pressure* [26]. The viscous stress has the usual form, with a viscosity that is proportional to T_g. The third relation [i.e., the second part of Eq. (4)] is from the balance equation for T_g, and valid only under stationary condition, when the production of granular jiggling (i.e., T_g) by a shear rate is equal to the rate at which T_g relaxes. The granular temperature T_g is then constant and given as $T_g \sim v_s = \dot\gamma$; see Eq. (9). (Note that the properly defined, invariant shear rate is v_s, while $\dot\gamma$ is the commonly used, though only loosely defined, notation, for the same quantity. We shall use them interchangeably in the introduction, but define $\dot\gamma \equiv \nabla_x v_y$ in Sec III.)

For given shear rates, π_{ij} assume the density-dependent critical form $\pi^{(c)}_{ij}(\rho)$, and $T_g \sim \dot\gamma$ holds. We therefore write the pressure $P \equiv \sigma_{\ell\ell}/3$ and a shear stress component as

$$P = P^{(c)}(\rho) + e_1(\rho)\dot\gamma^2, \tag{5}$$

$$\sigma_{xy} = \sigma^{(c)}_{xy}(\rho) + e_2(\rho)\dot\gamma^2. \tag{6}$$

For constant density, P and σ_{xy} are obviously monotonically increasing functions of the rate $\dot\gamma$. Keeping instead the pressure P constant, the density $\rho(P,\dot\gamma)$, obtained from inverting Eq. (5), becomes rate dependent. Inserting $\rho(P,\dot\gamma)$ into Eq. (6), monotonicity of σ_{xy}, depending on the specific form of $P^{(c)}(\rho), \sigma^{(c)}_{xy}(\rho), e_1(\rho), e_2(\rho)$, is frequently lost. These functions contain material parameters that are specified below. They have been obtained in previous works by comparison with experiments, especially in Refs. [16,19], since general principles do not put sufficient constraint on them. Given these expressions, GSH lets the density remain constant at slow rates (in the rate-independent regime), but it starts to decrease at higher ones, as a result of which the elastic contribution $\sigma^{(c)}_{xy}(\rho)$ decreases as well. For appropriate material parameters, this happens faster than the viscous term $e_1(\rho)\dot\gamma^2$ increases, such that the shear stress displays a dip. It is a dip because at yet higher rates, the viscous term always wins, and the shear stress grows without bounds.

Both cited experiments that have observed the stress dip have highly nonuniform density and shear rates. A quantitative comparison with GSH would therefore require the numerical solution of a large set of nonlinear, partial differential equations. Qualitatively speaking, however, because enforcing a constant volume does not prevent the local density to vary, a stress dip may still occur.

To understand this better, consider for simplicity two subvolumes (each uniform), in contact via a flexible membrane, such that the total volume $V_1 + V_2$ is a constant. This should serve as a model for the continuous nonuniformity of a constant volume experiment. Initially the total system is uniform, with both densities equal, $\rho_1 = \rho_2$, and both shear rates vanishing, $\dot\gamma_1, \dot\gamma_2 = 0$. Now, if $\dot\gamma_2$ is cranked up, but $\dot\gamma_1$ remains zero, because of pressure equality, $P_1(\rho_1,\dot\gamma_1) = P_2(\rho_2,\dot\gamma_2)$, the density must change and the membrane will stretch in one direction, with ρ_2 decreasing and ρ_1 increasing. If system 1 is much larger than 2, the stretching of the membrane will not change ρ_1 much, and as a result, $P_1(\rho_1,\dot\gamma_1)$ will remain essentially constant. $P_2 = P_1$ will as well, and the pressure-controlled limit holds in system 2. More realistically, in both experiments system 1 seems larger, but not by orders of magnitude. Then an intermediate case between the pressure- and density-controlled limits will happen. As only in the strictly density-controlled limit do we have monotonicity of the shear stress, any inhomogeneity of shear rates may result in nonmonotonic behavior of the shear stress; it is only a question of degree.

We summarize: A minimum of the shear stress as a function of the shear rate is forbidden in Newtonian fluids for general reasons, but was observed in granular media [1,2]. GSH, derived in explicit compliance with general principles, agrees with this observation: It strictly forbids a stress minimum for given density, independent of material parameters, but does allow it for given pressure, or any experimental setup such that the density changes with the rate. Employing parameters from previous works, validated using other experiments, and

assuming uniform state variables, we show in this paper that a stress minimum does occurs for given pressure. The experiments were performed at constant volume but with a spatially varying rate. The consideration of the last paragraph shows why a varying rate leads to a changing local density at constant total volume, hence making a stress minimum possible. More specifically, two subsystems in pressure equilibrium with constant total volume are considered, with only one being subject to a shear rate.

Our calculation below shows rise and drop of the density, as a function of the rate at given pressure, with one of the stronger drops taking place at the rate of the stress minimum. The experiments [1,2] show an increase of the volume, or average density, for given pressure at approximately the same rate (within an order of magnitude, the coordinates are logarithmic) where the stress minimum was observed for given volume. No information on what happens to the stress at given pressure is provided, though the average density of course cannot change at given volume. Now, even assuming both are correlated, there is less of a contradiction than it appears, because a shear band was consistently observed in the experiments [27], implying most of the shear rate is concentrated there. Since the solid regions outside the shear band sustain a vanishing shear rate, they do not participate in what GSH describes happens at elevated rates, but will massively contribute to the average density. Given the continuity of pressure, shear stress, chemical potential, etc., from the shear band to the solid region, it is clear that both densities are correlated. It is also quite conceivable that a density minimum in the shear band entails a maximum in the solid region. As a result, the average density goes up, although that in the shear band goes down.

II. THEORY

In this section GSH is presented in greater detail, with a focus on those expressions that were actually solved. The first two equations are conservation of density and momentum density:

$$\partial_t \rho + \nabla_i(\rho v_i) = 0, \tag{7}$$

$$\partial_t(\rho v_i) + \nabla_j(\sigma_{ij} + \rho v_i v_j) = 0. \tag{8}$$

As compared to Newtonian fluids, the additional variables of granular media are *granular entropy* s_g and the *elastic strain* u_{ij}. The first accounts for the energy contained in the mesoscopic, intergranular degrees of freedom such as the random, small-scaled motion of the grains. The elastic strain u_{ij} is the part of the strain that deforms the grains and gives rise to reversible storage of the elastic energy.

A two-stage irreversibility holds: Energy decays from the macroscopic to the mesoscopic degrees of freedom, and then to the microscopic, innergranular ones. Slowly varying stress or flow fields are macroscopic. Jiggling and sliding of the grains are mesoscopic, they are summarily quantified by granular entropy and temperature, s_g, T_g. Microscopic degrees of freedom such as phonons are quantified by the true entropy and temperature s, T. Energy never goes backwards: We cannot agitate granular medium by heating it, nor cause granular flow by T_g alone.

Given these inputs, GSH is set up by following the hydrodynamic procedure (see Ref. [28] for a pedagogical presentation and Ref. [16] for the actual execution): Maximizing the entropy with appropriate constraints, the equilibrium conditions and the associated thermodynamic forces are obtained. Then, starting from energy conservation, the reactive and dissipative fluxes for all state variables are derived. These are proportional to thermodynamical forces, with the coefficients given by the Onsager matrix. The product of fluxes and thermodynamical forces determines entropy production that is required to be positive definite and vanish in equilibrium.

The equation for the true entropy s is not needed for our purpose. The equation for the granular entropy s_g, closely related to the energy-density balance equation of Ref. [29], is

$$\begin{aligned} &T_g \partial_t s_g + T_g \nabla_i (s_g v_i - \kappa_g \nabla_i T_g) \\ &\quad = \kappa_g (\nabla T_g)^2 + \eta_g v_s^2 + \zeta_g (v_{ll})^2 - \gamma T_g^2, \end{aligned} \tag{9}$$

where $v_s^2 \equiv v_{ij}^0 v_{ij}^0$, T_g is the granular temperature, $\eta_g, \zeta_g > 0$ are, respectively, the shear and compressional granular viscosities and $\kappa_g > 0$ is the granular heat diffusion coefficient. The last term in Eq. (9), with the transport coefficient $\gamma > 0$, accounts for T_g relaxation, or the energy decay from mesoscopic to microscopic degrees of freedom. Note that the transport coefficients depend on the state variables, especially T_g and ρ. This we shall specify in the next chapter. (Note this γ is unrelated to the shear rate, conventionally denoted as $\dot{\gamma}$.)

When grains jiggle and slide, $T_g \neq 0$, they will briefly loose contact with one another. During this time, the deformation of the grains will decrease and the stored elastic energy will diminish. This is the reason granular media are *transiently elastic*, similar to polymers [16]. The difference is that the associated rates are proportional to T_g and not material constants; hence they vanish for $T_g = 0$ and become permanently elastic in this limit. So we take the elastic strain u_{ij} to increase with the shear rate v_{ij}, and to decrease by relaxation for finite T_g. In addition to geometric considerations, the equation of motion for u_{ij} is

$$\begin{aligned} &(\partial_t + v_k \nabla_k) u_{ij} - v_{ij} + u_{ik} \nabla_j v_k + u_{jk} \nabla_i v_k \\ &\quad = -\alpha_{ijkl} v_{kl} - u_{ij}^0 / \tau_0 - u_{ll} \delta_{ij} / 3\tau_1, \end{aligned} \tag{10}$$

$$1/\tau_0 = \lambda_0 T_g, \quad 1/\tau_1 = \lambda_1 T_g. \tag{11}$$

The last two terms of the first line are of geometric origin, and the last two terms of the second line are dissipative. The traceless part u_{ij}^0 and the trace of the elastic strain $\Delta \equiv -u_{ll}$, decay with different rates, where λ_0 and λ_1 depend on ρ. We conjecture that both relaxation rates vanish at the maximally possible density ρ_{cp}, the *random close packing* one. Hence we take $\lambda_0, \lambda_1 \propto (\rho - \rho_{cp})$.

The tensor α_{ijkl} is reactive and does not contribute to the entropy production. It has a counter term in the stress tensor that (according to Onsager relation) has an opposite sign, and the contribution of both to entropy production cancel. To first order in the strain, it is given by [24,30]

$$\alpha_{ijkl} = \alpha \delta_{ik} \delta_{jl} + \alpha_2 u_{kl}^0 \delta_{ij} / 3. \tag{12}$$

The tensor α_{ijkl} modifies the rate at which the elastic strain evolves for given shear rate. It also accounts for the softening of the medium with growing T_g. It is probably a result of force

chains being broken by the shear motion. Only by including α_2 (see Ref. [24]) is the so-called *critical state* (the perfectly plastic one characterized by a constant shear stress and density at given shear rate and pressure [31]) realistically accounted for. The stress tensor is

$$\sigma_{ij} = \pi_{ij} - \alpha_{klij}\pi_{kl} - \pi_{ik}u_{jk} - \pi_{jk}u_{ik} + P\delta_{ij} - \zeta_g v_{ll}\delta_{ij} - \eta_g v^0_{ij}. \tag{13}$$

The last two terms are dissipative and account for viscosity. The pressure P is given by the free energy $f(\rho, T_g, u_{ij})$ as $P \equiv \rho\partial f/\partial\rho - f$. It has two contributions, *seismic* and *elastic*:

$$f = f_T + f_{el}, \quad P = P_T + P_{el}, \tag{14a}$$

$$P_T = \rho\partial f_T/\partial\rho - f_T, \tag{14b}$$

$$P_{el} = \rho\partial f_{el}/\partial\rho - f_{el}, \tag{14c}$$

$$f_T = -\frac{1}{2}\rho b_0\left(1 - \frac{\rho}{\rho_{cp}}\right)^{0.1} T_g^2, \tag{14d}$$

$$f_{el} = \mathcal{B}\sqrt{\Delta}\left(\frac{2}{5}\Delta^2 + \frac{u_s^2}{\xi}\right). \tag{14e}$$

Note $u_s^2 \equiv u^0_{ij}u^0_{ij}$, and that b_0 is a dimensional constant which may be set to 1 by appropriately defining the dimension of T_g. The coefficient $\mathcal{B}$, accounting for overall rigidity, is

$$\mathcal{B} = \mathcal{B}_0\left(\frac{\rho - \bar{\rho}}{\rho_{cp} - \rho}\right)^{0.15}. \tag{15}$$

$\mathcal{B}_0$ is the rigidity coefficient and the parameter $\bar{\rho} \equiv (20\rho_{lp} - 11\rho_{cp})/9$. The expression for $\mathcal{B}$ delivers stable elastic solutions only for $\rho_{lp} \leqslant \rho \leqslant \rho_{cp}$, between the random loosest and closest packing density. There is no stable elastic solution for $\rho_{lp} > \rho$, because grains cannot stay static when they lose contact with one another. This built-in property of Eq (14e) is compatible with simply setting $\mathcal{B} = 0$ for $\rho \leqslant \rho_{lp}$.

Note that both exponents, 0.1 and 0.15, respectively, of Eqs. (14d) and (15), are approximate values taken from previous studies. As $\mathcal{B}$ falls to zero at $\rho = \rho_{lp}$, long before $\rho \to \bar{\rho}$, no limiting behavior is implied here. The same is true for the dense limit, because we take ρ_{cp} as the ideal density increasingly difficult to approach, at which there is no room left for any granular rearrangements or plastic motion.

The elastic stress π_{ij} is given as

$$\pi_{ij} \equiv -\frac{\partial f}{\partial u_{ij}} = \mathcal{B}\left[\sqrt{\Delta}\left(\Delta\delta_{ij} - \frac{2}{\xi}u^0_{ij}\right) + \frac{u_s^2}{2\xi\sqrt{\Delta}}\delta_{ij}\right]. \tag{16}$$

As the elastic energy f_{el} is convex with respect to u_s and Δ only for

$$\frac{u_s}{\Delta} \leqslant \sqrt{2\xi} \quad \text{or} \quad \frac{\pi_s}{\pi_{ll}/3} \leqslant \sqrt{\frac{2}{\xi}}, \tag{17}$$

where $\pi_s^2 = \pi^0_{ij}\pi^0_{ij}$, it contains the information of granular yield, e.g., that a layer of sand on an inclined plane may remain at rest only when the inclination angle is less than about 30°. That is the reason we take ξ as density independent and approximately $\xi = 5/3$.

All this is a brief presentation of the many considerations in Refs. [16,19,23], to obtain material-dependent parameters from various experiments. Refer to these references for more details.

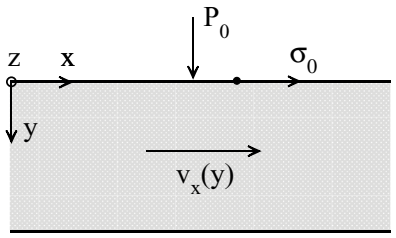

FIG. 1. Geometry of setup for the simple shear problem. Granular media is located between two plates. The upper plate is sheared with the shear stress σ_0, whereas the lower plate is at rest. The pressure P_0 is applied to the upper plate.

III. EQUATIONS FOR THE GEOMETRY OF SIMPLE SHEAR

We consider the simple shear geometry (see Fig. 1), aiming to find all *stationary, homogeneous* solutions. We search for solutions with a nonzero velocity component only along x, varying linearly along y, implying $\dot{\gamma} \equiv \partial_y v_x = \text{const}$. The elastic stress π_{ij} and the density ρ are constant as well. In addition, from the geometry, we can deduce $u_{yz} = u_{xz} = 0$. We choose the y axis downwards with $y = 0$ corresponding to the upper plate. In such a geometry, the shear rate is negative, $\dot{\gamma} < 0$. But in the figures below, the absolute value of $\dot{\gamma}$ will be plotted. In accordance with the assumptions above, $v_{ll} = 0$. The confining pressure applied to the upper plate P_0 is assumed to be much larger than the weight of the sand, so gravitation may be neglected.

Density and momentum equations. Since $v_y = v_z = 0$, $\rho = \text{const}$, and $v_x = v_x(y)$, Eq. (7) for the density is identically satisfied. From the momentum balance equation (8) follows that stress components must be constant everywhere within a granular layer:

$$\sigma_{xy} = \sigma_0, \tag{18a}$$

$$\sigma_{yy} = P_0, \tag{18b}$$

where σ_0 is the shear stress acting on the upper plate. Taking into account the definition for the stress tensor (13), we arrive at

$$\sigma_{xy} = (1-\alpha)\pi_{xy} - \left(\frac{2\alpha_2}{3} + 1\right)u_{xy}\pi_{xx} - \left(\frac{\alpha_2}{3} + 1\right)u_{xy}\pi_{yy} - \pi_{xy}(u_{xx} + u_{yy}) - \frac{\eta_g}{2}\dot{\gamma}, \tag{19a}$$

$$\sigma_{yy} = (1-\alpha)\pi_{yy} - \frac{2\alpha_2}{3}u^0_{yy}\pi_{xx} - \frac{\alpha_2}{3}u^0_{yy}\pi_{yy} - 2u_{xy}\pi_{xy} - 2\pi_{yy}u_{yy} + P. \tag{19b}$$

T_g equation. The transport coefficients η_g and γ which enter into Eq. (9) for granular entropy might be expanded with respect to T_g as [16]

$$\eta_g = \eta_1 T_g, \quad \gamma = \gamma_0 + \gamma_1 T_g, \tag{20}$$

where the zeroth order term in the expansion of η_g is missing to ensure the correct transition to the elastic limit and η_1 and

γ_1 are functions of ρ taken to be as [24]

$$\eta_1 = \frac{h_1 b_0^{1/2} \rho_{cp}}{(1-\rho_n)^{\beta+\varepsilon}}, \quad \gamma_1 = \frac{g_1 b_0^{3/2} \rho_{cp}}{(1-\rho_n)^{\beta}}, \tag{21}$$

where h_1, g_1, β, and ε are material parameters. In what follows the density is normalized to the *random close packing* density, $\rho_n = \rho/\rho_{cp}$.

Note also the divergent nature of the transport coefficients, which is a typical situation when approaching the maximal value for the density (see, e.g., Ref. [12]). It can be intuitively explained as follows. The larger the density is, the longer the grains are in contact with each other, leading to a more effective momentum and energy transfer, described by terms proportional to, respectively, η_g and γ. It is worth noting, that the shear rate $\dot\gamma$ appears in all terms together with a quantity $d = \sqrt{\eta_1\gamma_1}/\gamma_0$, which has a dimension of seconds. Thus, we believe that d determines the time scale and for the regimes considered below might be assumed to be independent on the density.

Next, we obtain the expression for stationary T_g as a function of the shear rate $\dot\gamma$ from Eq. (9):

$$T_g = \sqrt{\frac{\eta_1}{\gamma_1}} \cdot \frac{\Psi(\dot\gamma d)}{2d}, \quad \text{with} \quad \Psi(\dot\gamma d) = \sqrt{1+2(\dot\gamma d)^2} - 1. \tag{22}$$

Equations for u_{ij}. Writing explicitly expressions for all nonzero strain components the following expressions are derived from Eq. (10):

$$-(1-\alpha)\dot\gamma + \frac{2u_{xy}}{\tau} + 2u_{xx}\dot\gamma = 0, \tag{23a}$$

$$\left(\frac{\alpha_2}{3}+2\right)\dot\gamma u_{xy} + \frac{u_{yy}}{\tau} + \frac{\Delta}{3\tau_2} = 0, \tag{23b}$$

$$\frac{\alpha_2}{3}\dot\gamma u_{xy} + \frac{u_{xx}}{\tau} + \frac{\Delta}{3\tau_2} = 0, \tag{23c}$$

$$u_{zz} = u_{xx}, \tag{23d}$$

where $1/\tau_2 = 1/\tau - 1/\tau_1$. Substituting T_g given by Eq. (22) into Eq. (11) and using the definitions for the transport coefficients introduced in [24,30]:

$$\lambda_0 = \sqrt{\frac{\gamma_1}{\eta_1}}\tilde l_0(1-\rho_n), \quad \lambda_1 = \sqrt{\frac{\gamma_1}{\eta_1}}\tilde l_1(1-\rho_n), \tag{24}$$

the following expressions for the relaxation times are obtained:

$$\frac{1}{\tau_0} = \frac{\tilde l_0(1-\rho_n)}{2d}\Psi(\dot\gamma d), \quad \frac{1}{\tau_1} = \frac{\tilde l_1(1-\rho_n)}{2d}\Psi(\dot\gamma d), \tag{25}$$

where $\tilde l_0$ and $\tilde l_1$ are material parameters. Note that $1/\tau_0 \to 0$ and $1/\tau_1 \to 0$ as $\rho \to \rho_{cp}$ in accordance with the discussion above. The transport coefficient α_2 is taken to be as [24,30]

$$\alpha_2 = \kappa_2(1-\rho_n). \tag{26}$$

In summary, our problem consists of a set of nonlinear equations (18a)–(19b) and (23a)–(23d) with P, stress-strain relation, transport coefficients T_g, and relaxation times given by, respectively, Eqs. (14b), (14c), (16), (20), (26), (22), and (25). After some straightforward algebra we are finally faced with a set of four nonlinear algebraic equations with respect to $\dot\gamma$, ρ, π_{xy}, and π_{yy} which was solved numerically.

In calculations the following parameters were used: $\rho_g = 2970\ \mathrm{kg/m^3}$ (the grain density), $\rho_{cp} = 0.645\,\rho_g$, $\rho_{lp}/\rho_{cp} = 0.82$, $\bar\rho/\rho_{cp} = 0.667$, $\alpha = 0.7$, $\mathcal{B}_0 = 156$ MPa, $\tilde l_0 = 2850$, $\tilde l_1 = 855$, $\beta = 1$, $\kappa_2 = 750$, and $\varepsilon = 0$.

It is worth noting that h_1 has the dimension of length, whereas $h_1 g_1$ is dimensionless. Therefore, h_1 and g_1 could well be related to some geometric properties of the grains such as its form and diameter D, as well as the restitution coefficient r. Comparing our expression for the seismic stress to the corresponding expressions of Ref. [29], to lowest order in ρ, we indeed find $h_1 = \sqrt{\pi/4}\ D$ and $g_1 = \sqrt{\pi/6}(1-r^2)/D$, implying $h_1 = 3.4\times10^{-4}$ m for $D = 1.2$ mm and 4.7×10^{-4} m for 1.6 mm. (Reference [29] is a review of realistic two-dimensional models for dense granular media.)

A. Approximate model

Although our calculation is executed using the above complete expressions, we shall argue in the discussion below employing an approximate model, which is rather more simple and obtained under several assumptions. The first one is that all diagonal elements of the strain tensor u_{ij} are equal. The second assumption is that the zeroth order term γ_0 in the expansion of transport coefficient γ from Eq. (20) might be neglected, implying that $d \to \infty$. Note that γ_0 becomes significant only at very small shear rates corresponding to the *quasi-elastic limit* and, as will be shown later, bounds the *rate-independent regime* from below. In our derivations we keep the lowest order elastic terms which is the third simplification. Finally, the total shear stress and the pressure can be split as

$$P_0 = \sigma_{yy}^{(c)} + P_T, \tag{27a}$$

$$\sigma_0 = \sigma_{xy}^{(c)} + \sigma_{xy}^{(v)}, \tag{27b}$$

where $\sigma_{yy}^{(c)}$ and $\sigma_{xx}^{(c)}$ are the elastic contributions:

$$\sigma_{yy}^{(c)} = (1-\alpha)\mathcal{B}\sqrt{\Delta}\left(\Delta + \frac{u_s^2}{2\xi\Delta}\right), \tag{28a}$$

$$\sigma_{xy}^{(c)} = -\mathcal{B}\sqrt{\frac{\Delta}{2}}u_s\left[\alpha_2\left(\Delta + \frac{u_s^2}{2\xi\Delta}\right) + \frac{2}{\xi}(1-\alpha)\right], \tag{28b}$$

and P_T and $\sigma_{xy}^{(v)}$ are, respectively, the T_g-generated, *seismic pressure* and the *viscous shear stress*

$$P_T = \frac{\rho_{cp}}{40}\frac{h_1}{g_1}\frac{\rho_n^2\dot\gamma^2}{(1-\rho_n)^{9/10+\varepsilon}}, \tag{29a}$$

$$\sigma_{xy}^{(v)} = \rho_{cp}\sqrt{\frac{h_1^3}{8g_1}}\frac{\dot\gamma^2}{(1-\rho_n)^{\beta+3\varepsilon/2}}. \tag{29b}$$

The elastic shear strain and compression are mere functions of the density and transport coefficients and are

$$u_s \simeq \frac{1-\alpha}{\tilde l_0(1-\rho_n)}, \quad \Delta \simeq \frac{\kappa_2}{\tilde l_1}u_s. \tag{30}$$

IV. DISCUSSION

In our calculations we consider a *pressure-controlled* system keeping the pressure at the top $P_0 = 10$ kPa and varying the shear rate $\dot\gamma$. The results of calculations are shown

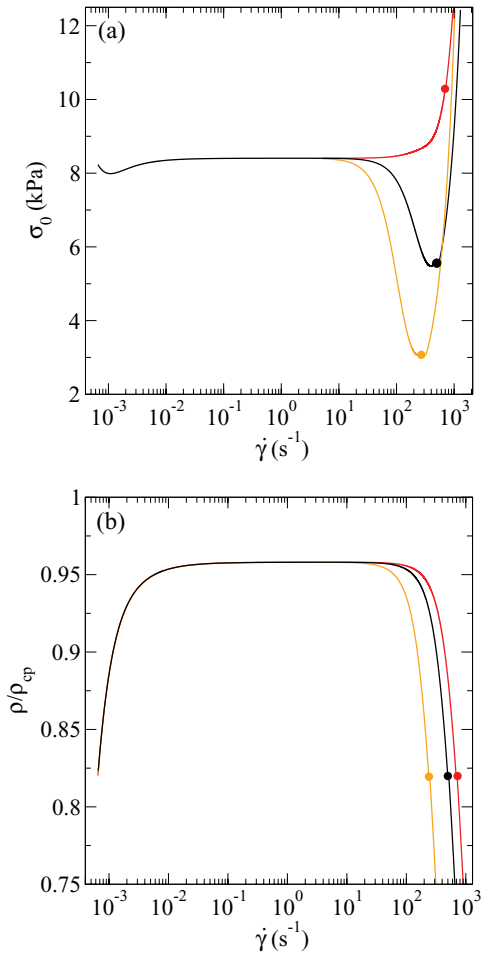

FIG. 2. (Color online) Shear stress σ_0 (a) and density ρ (b) vs shear rate $\dot\gamma$ for $P_0 = 10$ kPa and different material parameters g_1, h_1: $g_1 = 3.6$ m^{-1}, $h_1 = 4.7 \times 10^{-4}$ m (red [dark gray]); $g_1 = 1.4$ m^{-1}, $h_1 = 3.4 \times 10^{-4}$ m (black); $g_1 = 0.32$ m^{-1}, $h_1 = 3.4 \times 10^{-4}$ m (orange [light gray]). Above some critical values for the shear rates (shown by filled circles), the density $\rho < \rho_{lp}$, and, as a result, there are no elastic contributions. The values for the inertia number $I = \dot\gamma D/\sqrt{P_0/\rho_g}$ [15] are estimated to be 0.60, 0.33, and 0.18 at the critical values designated by, respectively, red (dark gray), black, and orange (light gray) filled circles.

in Figs. 2 and 3 where the shear stress σ_0 and the density ρ are plotted as a function of the shear rate $\dot\gamma$. We can distinguish between three different regimes, which are summarized below.

A. Rate-independent regime

The rate-independent regime is characterized by almost unchanged σ_0, ρ_n, and u_{ij} upon variation of $\dot\gamma$ by a few orders of magnitude [plateaus in Figs. 2(a) and 2(b)]. Moreover, within this stationary regime the elastic terms, $\sigma^{(c)}_{yy}$ and $\sigma^{(c)}_{xx}$, give dominant contribution, so that the seismic pressure P_T and the viscous shear stress $\sigma^{(v)}_{xy}$ might be neglected, leading to

$$P_0 = \sigma^{(c)}_{yy}, \tag{31a}$$

$$\sigma_0 = \sigma^{(c)}_{xy}. \tag{31b}$$

Each point of the plateaus corresponds to the *critical state* which is a stationary solution of the evolution equations for the

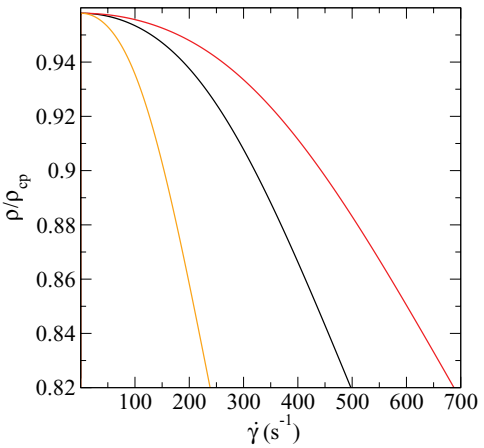

FIG. 3. (Color online) Density ρ from Fig. 2(b) versus shear rate $\dot\gamma$ in lin-lin plot. Here only parts of the solutions with $\rho > \rho_{lp}$ are depicted.

elastic strain. We estimate at which σ_0 and ρ_n for a fixed value of P_0 the rate-independent regime sets in. For this purpose we insert the expressions (30) for u_s and Δ into Eqs. (28a) and (28b) and solve a resulting set of two algebraic equations (31a) and (31b) with respect to σ_0 and ρ_n. We found $\sigma_0 \simeq 8.3$ kPa and $\rho_n \simeq 0.96$, which is in a perfect correspondence with the exact numerical calculations [compare with the values of plateaus shown in Figs. 2(a) and 2(b)].

Remarkably, the rate-independent regime is energetically stable in a sense of the criteria (15,17). However, at some lower shear rates the density drastically decreases with $\dot\gamma$, and a solution becomes finally unstable [no solutions below a certain $\dot\gamma$ in Figs. 2(a) and 2(b)]. It is worth noting that the value of d bounds the rate-independent regime from below that is captured by the exact numerical calculations only.

B. Rapid flow (Bagnold) regime

The rapid flow regime takes place at high values of shear rates, $\dot\gamma \geqslant 300\,Hz$ [see Fig. 2(a)] and is characterized by a quadratic growth of the shear stress σ_0 with $\dot\gamma$. Indeed, in the limit of large shear rates the viscous and seismic terms prevail over the elastic ones, so that we can write

$$P_0 = P_T, \tag{32}$$

$$\sigma_0 = \sigma^{(v)}_{xy}. \tag{33}$$

Note that Eqs. (32) and (33) are exact when $\rho < \rho_{lp}$ since elastic contributions become energetically unstable as was discussed before. Thus, we obtain a typical stress-shear relationship for the rapid flow, $\sigma_0 \sim \dot\gamma^2$, the so-called *Bagnold scaling* [32].

Dividing the right- and left-hand sides of Eq. (32) by the right- and left-hand sides of Eq. (33), respectively, a simple algebraic equation for the density ρ_n can be derived. The expressions for u_s and Δ are again given by Eqs. (30). However, the elastic contributions (when present) are much smaller than that within the rate-independent regime where the density reaches its highest possible value [plateaus in Fig. 2(b)].

C. Transient regime

The transient regime occurs at moderate shear rates and is located between the rapid flow and the rate-independent regimes. We refer to it as to transient because all contributions from elastic, viscous, and seismic terms are essential, and none of them can be neglected. It is seen that a shear stress might exhibit an unexpected dip with increasing shear rate that looks counterintuitive at a first sight. This can be explained as follows. As before, we split contributions to σ_0 into two parts, elastic and viscous ones, writing symbolically $\sigma_0 = \sigma_{xy}^{(c)} + e_1\dot{\gamma}^2$. Let us start from the rate-independent regime for which $\sigma_0 \simeq \sigma_{xy}^{(c)}$. As a shear rate increases, the viscous contributions start to play a role turning a functional dependence of σ_0 towards $e_1\dot{\gamma}^2$. However, this route is accompanied by a drastic decrease of the density leading to diminishing contributions from the elastic terms in accordance with Eq. (30). The steeper the density decrease, the more rapidly elastic contributions vanish. In two of three examples presented in Fig. 2 such an abrupt density decrease [see Fig. 2(b)] leads to the dip in the shear stress because the diminishing contribution of the elastic terms is not compensated by the quadratically grown viscous terms within this interval of the shear rates. With further increase of $\dot{\gamma}$, the viscous contributions become more significant as compared to the elastic ones, which finally vanish due to energetic instability and a system switches to the Bagnold regime, for which $\sigma_0 = e_1\dot{\gamma}^2$.

In further study we explored the system's response upon variation of different material parameters and realized that the dependence $\sigma_0(\dot{\gamma})$ shown in Fig. 2(a) is qualitatively rather universal. We found that the plateaus, representing the rate-independent regime, can easily be extended towards smaller and/or larger values of the shear rates, and the value of a dip can also be easily regulated or suppressed. It is worth noting that we can reproduce our curve $\sigma_0(\dot{\gamma})$ to a rather good accuracy using the empirical formula (1) from Ref. [2] adapting the fitting parameters accordingly.

V. CONCLUSIONS AND OUTLOOK

In this paper we analyzed all stationary homogeneous solutions in the simple shear geometry using the theory of granular solid hydrodynamics. We demonstrated the existence of three different regimes, namely, the rate-independent, transient, and rapid flow regimes, which appear subsequently as the shear rate is increased starting from low values. In particular, as a natural consequence of our equations we found a dip in the shear stress-rate functional dependence, recently revealed in the experiments dealing with top-rotating torsional shear cell. Such a counterintuitive dependence is related to the fact that elastic contributions start to decrease drastically (owing to a density decrease) when the shear rate reaches a certain value.

[1] K. Lu, E. E. Brodsky, and H. P. Kavehpour, J. Fluid Mech. **587**, 347 (2007).

[2] K. Lu, E. E. Brodsky, and H. P. Kavehpour, Nature Lett. **4**, 404 (2008).

[3] J. A. Dijksman, G. H. Wortel, L. T. H. van Dellen, O. Dauchot, and M. van Hecke, Phys. Rev. Lett. **107**, 108303 (2011).

[4] P. Wroth and A. Schofield, *Critical State Soil Mechanics* (McGraw-Hill, London, 1968).

[5] R. M. Nedderman, *Statics and Kinematics of Granular Materials* (Cambridge University Press, Cambridge, 1992).

[6] D. M. Wood, *Soil Behaviour and Critical State Soil Mechanics* (Cambridge University Press, Cambridge, 1990).

[7] D. Kolymbas, *Introduction to Hypoplasticity* (Balkema, Rotterdam, 2000).

[8] W. Wu and D. Kolymbas, *Constitutive Modelling of Granular Materials* (Springer, Berlin, 2000).

[9] G. Gudehus, *Physical Soil Mechanics* (Springer, Berlin, Heidelberg and New York, 2010).

[10] P. Schall and M. Hecke, Annu. Rev. Fluid Mech. **42**, 67 (2010).

[11] S. P. Pudasaini and K. Hutter, *Avalanche Dynamics* (Springer, Berlin, Heidelberg and New York, 2007).

[12] L. Bocquet, W. Losert, D. Schalk, T. C. Lubensky, and J. P. Gollub, Phys. Rev. E **65**, 011307 (2001).

[13] G. MiDi, Eur. Phys. J. E **14**, 341 (2004).

[14] P. Jop, Y. Forterre, and O. Pouliquen, Nature Lett. **441**, 727 (2006).

[15] Y. Forterre and O. Pouliquen, Annu. Rev. Fluid Mech. **40**, 1 (2008).

[16] Y. M. Jiang and M. Liu, Granular Matter **11**, 139 (2009); in *Mechanics of Natural Solids*, edited by D. Kolymbas and G. Viggiani (Springer, Berlin, Heidelberg and New York, 2009), pp. 27–46.

[17] D. O. Krimer, M. Pfitzner, K. Bräuer, Y. Jing, and M. Liu, Phys. Rev. E **74**, 061310 (2006).

[18] K. Bräuer, M. Pfitzner, D. O. Krimer, M. Mayer, Y. Jiang, and M. Liu, Phys. Rev. E **74**, 061311 (2006).

[19] Y. M. Jiang and M. Liu, Eur. Phys. J. E **22**, 255 (2007).

[20] Y. M. Jiang and M. Liu, Phys. Rev. E **77**, 021306 (2008).

[21] Y. M. Jiang and M. Liu, Phys. Rev. Lett. **93**, 148001 (2004).

[22] M. Mayer and M. Liu, Phys. Rev. E **82**, 042301 (2010).

[23] Y. M. Jiang and M. Liu, Phys. Rev. Lett. **99**, 105501 (2007).

[24] S. Mahle, Y. Jiang, and M. Liu, arXiv:1006.5131v3 [physics.geo-ph] (2010).

[25] S. Mahle, Y. Jiang, and M. Liu, arXiv:1010.5350v1 [cond-mat.soft] (2010).

[26] G. Gudehus, Y. M. Jiang, and M. Liu, Granular Matter **1304**, 319 (2011).

[27] Nicholas J. van der Elst (private communication); see also N. J. van der Elst, E. E. Brodsky, P.-Y. Le Bas, and P. A. Johnson (unpublished).

[28] P. M. Chaikin and T. C. Lubensky, *Principles of Condensed Matter Physics* (Cambridge University Press, Cambridge, 1995).

[29] S. Luding, Nonlinearity **22**, R101 (2009).

[30] S. Mahle, Ph.D. thesis, University Tuebingen, Germany, 2012.

[31] A. Schofield and P. Wroth, *Critical State Soil Mechanics* (McGraw-Hill, London, 1968); D. M. Wood, *Soil Behavior and Critical State Soil Mechanics* (Cambridge University Press, Cambridge, 1990).

[32] R. A. Bagnold, Proc. R. Soc. London A **255**, 49 (1954).